7-2013

Characterization of Polyamide-12; Hydrolysis Kinetics Comparison, and the Study of Crude-oil Pipeline Applications

Charles J. Blevins
College of William and Mary

Follow this and additional works at: https://scholarworks.wm.edu/honorstheses

Characterization of Polyamide-12; Hydrolysis Kinetics Comparison, and the Study
of Crude-oil Pipeline Applications

Charles Joseph Blevins

Bachelor of Science, The College of William and Mary, 2013

A Senior Honors Thesis presented for a Bachelor of Science Degree in Chemistry from the College
of William and Mary
Honors Thesis

Department of Chemistry

The College of William and Mary
May, 2013

APPROVAL PAGE

This Thesis is submitted in fulfillment of
the requirements for Honors in Chemistry; Bachelor of Science Degree

Charles Joseph Blevins

Approved by the Committee, May, 2013

Committee Chair
David Kranbuehl, Chemistry
The College of William and Mary

Deborah C. Bebout, Chemistry

Michael J. Pacella, Philosophy

ABSTRACT

Polyamides are one of the most widely used thermoplastics in the world due to their strength, toughness, stiffness, abrasion resistance, and retention of physical and mechanical properties over large temperature ranges. They are of extreme importance in a variety of industrial fields such as crude-oil transport in deep water environments, transport of natural gas, automobile applications in fuel lines, etc. Thus, research on the changes in their molecular and mechanical properties during aging in varying environments is important. The research herein examines the aging of two polyamide polymers, PA-11 and PA-12, and the resulting changes in their molecular and performance properties at different temperatures, in anaerobic environments, and neutral pH. The specific objective of this research is to observe the changes in the molecular weight, chain length, during the aging of the two polyamides to form a comparison between general amide bond hydrolysis kinetics for PA-11 vs. PA-12.

Acknowledgements

Professor David Kranbuehl

John-Andrew Samuel Hocker

Professor Deborah Bebout

Professor Michael Pacella

Dr. Arthur Jaeton Mitman Glover

Chemistry Department at the College of William and Mary

Roy Charles Center

Friends, Family, and Colleagues in Lab

Contents

Chapter

Tables

Table

Figures

Figure

Chapter 1

Introduction

Beginning in 2003, Wellstream International, in an effort to expand their supply of polymer pipeline materials, introduced poly-amide 12 (PA-12) as a viable addition to the polymer pipeline community. The idea behind this move by Wellstream focused on expanding the application of nylon (poly-amide) grades for off-shore applications in order to move away from a single supply source.(2) Prior to 2003, Wellstream International, and other companies, used poly-amide 11 (PA-11), seen in Figure 1.1, almost exclusively for the construction of riser and flow pipelines for deep-water off-shore drilling of crude oil. The PA-11 layer of the riser serves as a flexible liquid barrier for the crude, allowing the riser to flex without breaking, and also preventing the crude from entering the ocean environment. A depiction of the riser layers can be seen in Figure 1.2. PA-11 has been the industry standard for more than 30 years. However, the recent push to expand supply sources, especially with regard to PA-12, has raised many questions about the similarities between these two poly-amide polymers separated by only one alkane unit.

The initial report by Wellstream International, in 2007, suggested that PA-12 outperformed PA-11 in long range aging studies, and cited particular gains with respect to PA-12's aging in air (oxidative) environments in comparison to PA-11. In the past, PA-12 has not been used in large diameter pipeline applications due to its low melt viscosity. However, the particular grade of PA-12 examined by Wellstream, which represented a collaboration between Wellstream and Degussa AG, was shown "to increase its molecular weight during processing, in a controlled manner." This increase in molecular weight, from a solution viscosity of 2.1 to 2.4 (or higher), suggested that

Figure 1.1: Poly-amide-11 Structure

maybe PA-12 could be use in large diameter pipelines. In a report by Degussa AG, the third largest chemical company in Europe, results suggested that the new PA-12 VESTAMID LX9020 grade had specific advantages over the current polymer sources. The advantages include higher maximum operation temperatures (MOT) than PA-11, better processability than PA-11, and longer lifetime than PA-11. This new grade, VESTAMID LX9020, because of its high melt stiffness and hydrolysis resistant properties makes it ideal for large diameter pipe used in flexible crude oil riser pipelines. It is important to note that in this research, Wellstream used the industry standard Corrected Intrinsic Viscosity (CIV) values for PA-11, 1.2dl/g, as the accepted value for the design factor of PA-12; the point at which PA-11 is considered no longer safe for pipeline applications (2).

However, other researchers have since suggested that PA-12 might not be as promising as once thought. In 2009, the research group of Hochstetter et al. displayed evidence that PA-12 did not perform as well as Wellstream claimed in their initial report. The proposition by Hochstetter et al. centers around the idea that the CIV value of 1.2 dl/g, accepted by Wellstream as a valid design standard from their work with PA-11, is not applicable for use with PA-12. Their research suggests that "for any new poly-amide, the time to reach CIV of 1.2 dl/g cannot be considered as a sufficient design factor" without a more thorough characterization of the mechanical behavior of the polymer in relation to the aging time and temperature, as well as the molecular weight. The Hochstetter group experimented with a high molecular weight grade PA-12 with 8% plasticizer and 5% EPDM (impact modifier). This is not the same grade tested by Wellstream in collaboration with Degussa

Figure 1.2: Sample of NKT PA-11 pipeline. PA-11 layer of the pipeline is labeled 2.(1)

AG. (3)

However, the dispute that exists between these two factions is not so much a dispute over who is right, or whose PA-12 grade is better, but rather a dispute about what is best for the environment and society in regard to the safety of these pipelines. Hochstetter's research cites his specific results with a high molecular weight PA-12 grade polymer, and he suggests that the design standards for PA-11 and PA-12 should not be considered equivalent. This would only have implications in regard to the Wellstream research if in fact Hochstetter's results were reproducible in the new PA-12 VESTAMID LX9020 grade. At first glance, this does not seem to be the case, however the important take-away from this contradiction is that without extensive testing, no polymer can be considered to respond to stress and aging in the same way.

In the wake of the 2010 Deepwater Horizon oil spill in the Gulf of Mexico, the impacts of a deepwater drilling accident were brought to the global stage. A great deal of resources have been aimed at further research and development of these applications for future used. As discussed by both Glover and Hocker, the use of poly-amides in deep water drilling risers and flow pipelines is paramount to the function and safety of the pipelines. (1; 4) In addition to uses in the crude oil industry, PA-12 is already approved and used in fuel lines and air brake systems on over twenty-five auto manufacturers that include Audi, Ford, and General Motors. The golden age of polymer science is still in front of us, and research to understand new polymer grades and further the field of polymer chemistry could prove invaluable, solving many problems of engineering in society today.

In a report released in 2012, the International Energy Agency (IEA) predicted that the United States will be the world's largest producer of oil by the year 2020. The report suggests that the United States' production will peak at a volume of 11.1 million barrels of oil per day in the year 2020, all a part of the US's strategy to be energy independent in the changing global economy. This prediction is not only promising for the creation of jobs and engery independence for the US, but also depicts a reversal of the trend that the US has followed for decades, with large dependence on foreign oil and energy sources. However, this increase in production, heavily focused on off-shore deep-water drilling, relies heavily on the safety of these drilling techniques and equipment in

the harsh off-shore environments. (5) Thus, if PA-12 is going to be used in pipeline applications, further characterization of its properties is not just encouraged, it is of critical importance. It is evident that the research conducted on PA-12 is still in the early stages of characterization, and for that reason, it is our goal to further characterize this polymer, paying special attention to the mechanical properties of PA-12 throughout accelerated aging experiments. Our research aims to age PA-12 in three temperature environments, 80°C, 100°C, 120°C, all in de-oxygenated water.

There is a great deal of research that describes the hydrolysis of polyamides in solution and vapor phases, but the importance of this solid state hydrolysis chemistry is of increasing importance as off-shore drilling is pushed into deeper and deeper waters. "The drilling industry continues to move toward deeper waters and new deposits. In the Gulf of Mexico, drilling is now occurring beneath as much as 8,000 to 9,000 feet of water; the Deepwater Horizon rig, by contrast, was drilling in about 5,000 feet of water in the gulf when it exploded after a blowout nearly three years ago" (6). Our work is aimed at developing a greater understanding of the solid state hydrolysis of both polyamide 11 and 12. We are particularly interested in how the rate of hydrolysis changes between PA-11 and PA-12 polymer grades in the same environment. We hope to characterize the implications of different rates of hydrolysis by designing experiments testing both mechanical and chemical properties of the two polymers. Specific questions focus on how differences in crystallinity and structure change the rate of hydrolysis, and further, how differences relate to the activation energy of hydrolysis. It is our hypothesis, that because PA-12 has less uptake of water than PA-11 (7; 8), PA-12 will undergo a slower rate of hydrolysis than PA-11 under the same conditions. We aim to further characterize PA-12, in comparison to PA-11, in particular looking at the activation energy of hydrolysis, and the differences in crystallinity as they relate to the mechanical properties of PA-12.

Chapter 2

Instrumentation

2.1   Size Exclusion Chromatography - Multiple Angle Laser Light Scattering

Size Exclusion Chromatography (SEC) is used to fractionate the dissolved polymer sample by relative hydrodynamic volume. Multiple Angle Laser Light Scattering (MALLS) is used in complement to SEC, and is the primary method for determining the weight average molecular weight (M_W) of a given polymer sample. SEC-MALLS, measures the weight average molecular weight (M_W) of a polymer sample by fractionating the polymer sample based on chain length and monitoring the intensity of light scattered for each fraction.

2.1.1   Theory

Size Exclusion Chromatography separates polymer fractions by their specific hydrodynamic volume. The SEC is conducted using a high performance liquid chromatography system (HPLC) that houses three in-line Shodex Gel Permeation Chromatography (GPC) SEC columns. (Shodex: GPC Hexafluoro-2-propanol (HFIP)-803, GPC HFIP-805, GPC HFIP-LG). These columns are packed with a small polymer bead stationary phase, polystyrene-divinylbenzene copolymer beads, selected by their compatibility with the solvent being used, HFIP, and the polymer sample being analyzed. (9)

Each of the three columns is packed with a slightly different stationary phase, as indicated by the different model numbers represented above. The first column, packed with HFIP-LG performs very little separation, and is instead used to trap any contaminant or foreign substance prior to

the separation columns and MALLS instrument. The second column, packed with HFIP-805, has beads that separate at a 4 x 10^6 g/mole polystyrene exclusion limit. The last column, HFIP-803, separates at the 7 x 10^4 g/mole polystyrene exclusion limit, a limit that is smaller than the previous column. (9) These separation columns are used to provide known retention times of a standard polymer sample, which can be used to calibrate the MALLS instrument.

As the sample moves through the column, the small chain lengths take a path that runs through the bead stationary phase in a convoluted manner. However, the larger chain length pieces cannot fit through the small perforations in the stationary phase, and thus move in a path around the beads. In this manner, the larger pieces elute first, and the smaller pieces elute last. Once eluted from the SEC columns, the polymer sample enters the MALLS instrument, which measures the light scattered by each polymer fraction, from three different angles. The MALLS instrument takes data of light scattered at three different angles and pairs that with the concentration of the given fraction, determined by the RI detector using the $\frac{dN}{dc}$ calibration. Combined, this data is used to extrapolate the molecular weight of the polymer fraction using a Debye Plot. Once the entire sample has eluted, the weight average molecular weight of all the fractions can be determined. (10)

2.1.2   Sample Preparation

MALLS solutions are made by dissolving a small polymer sample in HFIP. The polymer sample is first dried for one hour at 100°C, to drive off any water absorbed from the environment. The sample is then massed to the nearest tenth of a milligram, 10^{-4} g, and added to the HFIP solvent. A simple calculation determines the amount of HFIP to add by mass to reach a polymer concentration of 2 mg/mL in solution. Once dissolved, after approximately one hour, 100μL of the polymer solution is injected into the SEC-MALLS apparatus, Figure 2.1.

The SEC and MALLS signals are interpreted using Wyatt Technologies' ASTRA software, and the data file produced is worked up using a custom MATLAB program written by J.A. Hocker. The MATLAB program plots raw voltage versus elution volume, see Figure 2.2. Selected peaks are normalized and integrated to determine molecular weight.
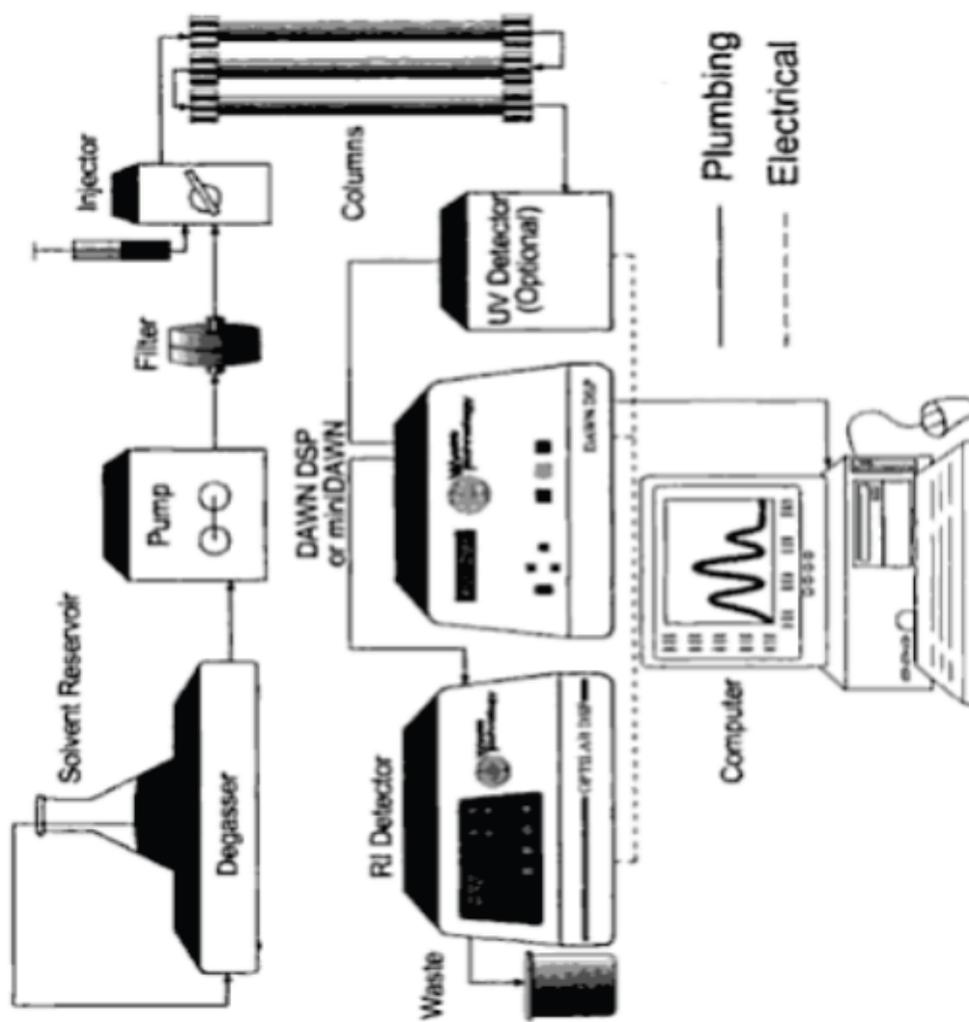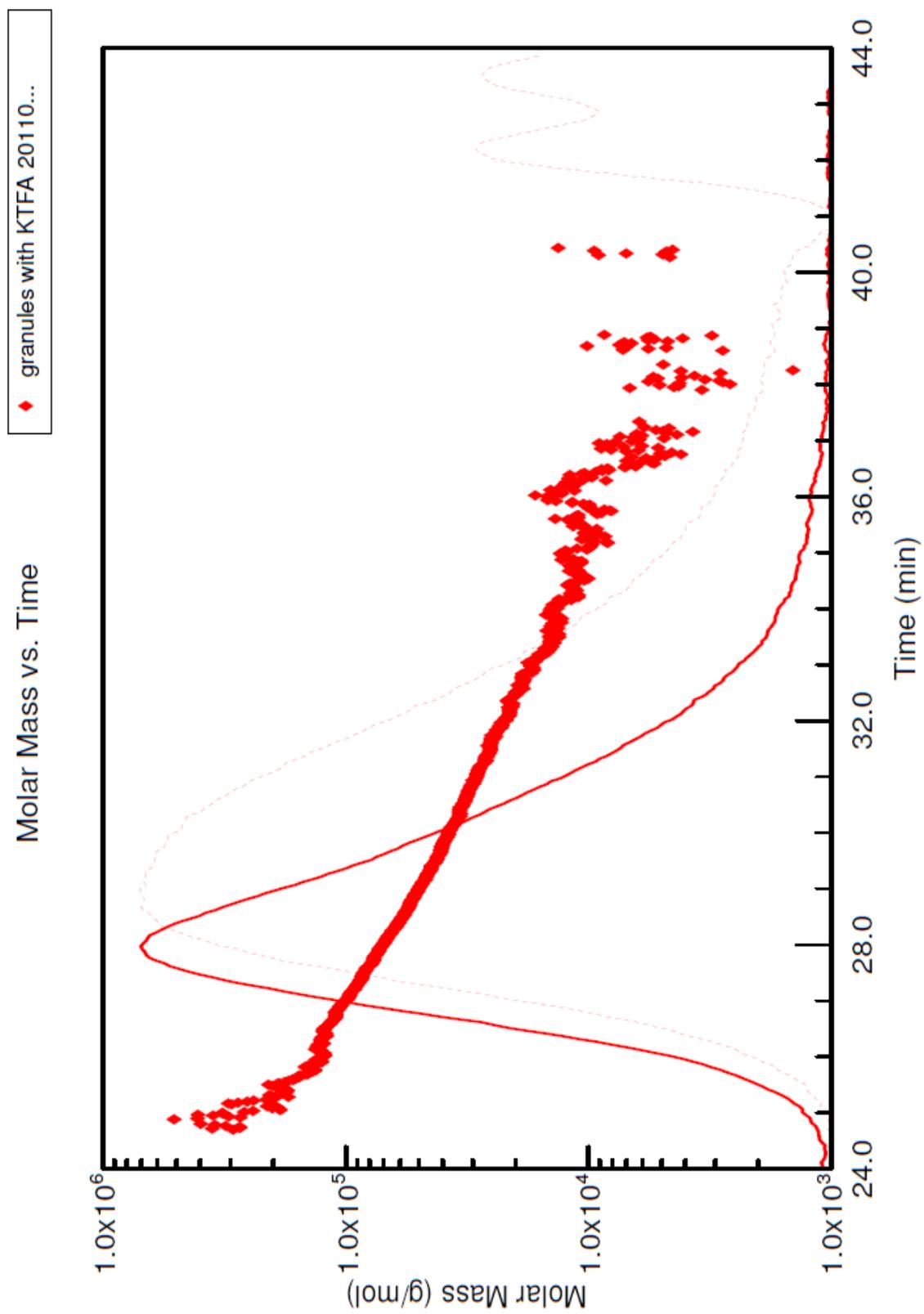
Figure 2.1: MALLS Schematic

Figure 2.2: MALLS Example Plot

2.2   Corrected Intrinsic Viscosity

A secondary method of determining a polymer sample's molecular weight, viscosity measurements take advantage of the relationship between solution viscosity and relative hydrodynamic volume of a polymer chain in solution. Secondary methods provide polymer chemists a quick, simple, and efficient way for calculating molecular weight, however, unlike MALLS, viscosity is not absolute method. Viscosity measurements are instead linked to molecular weight empirically using primary methods of calibration.

2.2.1   Theory

Polymer chains form colloidal suspensions in solution, and are best represented by randomly coiled chains, not ordered rods. The explanation for this phenomena comes from the interaction between polymer and solvent. The quality of a solvent is determined by its affinity for the solute. In a good solvent, the polymer chain interacts with the most solvent molecules possible; which Allcock described as a "saturated sponge." In this case, the single chain polymer interacts with solvent molecules at every possible location, thus expanding the single chain hydrodynamic volume drastically. This larger hydrodynamic volume is responsible for the increase is solution viscosity, and can be related empirically to the molecular weight of each chain. Thus, chemists can determine molecular properties using viscosity measurements. These measurements are derived from Einstein's work with colloidal suspensions in which he observed that "large particles in colloidal solutions tend to impede the flow of adjacent layers of liquid when the liquid is subjected to a shearing force." (10) One can measure the increased viscosity of a polymer solution relative to the pure solvent to determine molecular properties. It makes sense that the larger the polymer monomer, the larger the colloidal particle, and thus higher viscosity; but, the correlation between the relative viscosity and molecular weight of the monomer is much more complicated mathematically.

The relative viscosity of a solution, η_r, is represented by the time a polymer solution takes to move through the viscometer tube, t, and the time it takes pure solvent to move through the same viscometer under the same conditions, t_0. This ratio is equivalent to the viscosity of the solution,

η, to the viscosity of the pure solvent, η_r, as defined by Einstein's work with colloidal suspensions.

$$\eta_r = \frac{\eta}{\eta_0} = \frac{t}{t_0}. \tag{2.1}$$

In terms of relative viscosity, values of $\eta_r = 1.2$ - 1.8 are considered experimentally valuable, as it is difficult to measure changes in viscosity below twenty percent and above eighty percent. For this reason, a second term, specific viscosity, η_{sp}, is used to define the fractional increase in viscosity caused by the addition of a polymer sample to a solvent solution.

$$\eta_{sp} = \frac{\eta - \eta_0}{\eta_0} = \eta_r - 1 \tag{2.2}$$

There is a direct relationship between the specific viscosity, η_{sp}, and the concentration, c, of a polymer solution that can be represented by the reduced specific viscosity, $\frac{\eta_{sp}}{c}$. The relationship is plotted as $\frac{\eta_{sp}}{c}$ vs. c, and from this plot, the intrinsic viscosity, $[\eta]$, can be determined. The intrinsic viscosity is defined as the reduced specific viscosity at zero concentration. This extrapolation is used because there are many polymer chains that affect the solution viscosity at a given concentration. In order to gain the best representation of the change in viscosity upon the addition of one chain, the intrinsic viscosity is represented by y-intercept of the plot of $\frac{\eta_{sp}}{c}$ vs. c, the reduced specific viscosity at zero concentration. The intrinsic viscosity is modeled by Equation 2.3.

$$[\eta] = \lim_{c \to 0} \frac{\eta_{sp}}{c} \tag{2.3}$$

Once the intrinsic viscosity is determined, chemists use the Mark-Houwinck equation, Equation 2.4, to model the relationship between the intrinsic viscosity of a polymer solution and its viscosity average molecular weight. The molecular weight determined by the Mark-Houwinck relationship and viscosity measurements is called the viscosity molecular weight. Due the the nature of secondary calculations, the determination of viscosity molecular weight must be calibrated using a primary method such as light scattering or osmotic pressure. This calibration is represented in the equation where K and α are constants specific to a polymer solvent pair at a given temperature. Once calibrated, this method allows for simple, accurate, and quick determination of viscosity molecular weight values of a polymer sample in solution.

$$[\eta] = K M_v^{\alpha} \tag{2.4}$$

A more efficient method is corrected intrinsic viscosity (CIV), where the concentration of the solution is adjusted to account for the contribution of volatiles and plasticizer in a given polymer. The method of determining CIV values for polymer samples is standard procedure in industry and widely used to detect changes in molecular weight with degradation. The CIV is an adaptation of the Kramer relationship.

$$CIV = \ln\left(\frac{\eta_r}{C}\right) \tag{2.5}$$

$$C = c(1 - v) \tag{2.6}$$

In our methods, a polymer solution has a concentration of 5 mg/ml of polymer in meta-cresol. The corrected intrinsic viscosity calculation adjusts concentration by subtracting out the volatile fraction of the polymer sample. This volatile fraction is determined by thermogravimetric analysis (TGA), and contains water and plasticizer. Normal values for the volatile fraction range anywhere from 8% to 15% of the total polymer mass. The CIV value can be used to accurately assess molecular weight degradation of poly-amides.

2.2.2   Sample Preparation

Polymer solutions used for CIV measurement are made by dissolving small amounts of polymer in 3-methylphenol (meta cresol or m-cresol). The polymer samples are chopped into fine pieces to increase surface area and speed up the dissolving process. Before these chopped pieces are introduced to solvent, they are heated at 100°C in an oven for one hour to drive off any absorbed water in the sample. Once dried, the sample is massed, recorded, and added to the m-cresol solvent. A simple calculation determines the amount of m-cresol to be added, by mass, in order to achieve a 5 mg/mL solution concentration. Once the polymer is dissolved, the solution is ready for viscosity measurements. Due to the nature of colloidal suspension and solution viscosity, a small concentration of polymer can yield large fluctuation is solution viscosity, thus a concentration of 5 mg/mL was chosen. When experimenting with new polymer grades, varying solution concentrations are measured to verify/quantify the relationship between solution concentration and relative viscosity, which is used to determine intrinsic viscosity.

For the purpose of CIV measurements, the size of the viscometer capillary is imperative to getting accurate results. Given the viscosity of m-cresol at room temperature, approximately 20°C, a size 2 Ubbelohde viscometer is used for viscosity measurements, see Figure 2.3 for viscosity apparatus. Viscosity is a temperature dependent process, so all measurements are taken in a water bath heated/cooled to 20°C. Before a polymer solution is run, a fresh m-cresol run is made to determine t_0. Once the fresh times are established, the polymer solution is run and compared to the fresh m-cresol times. This comparison is defined as relative viscosity.
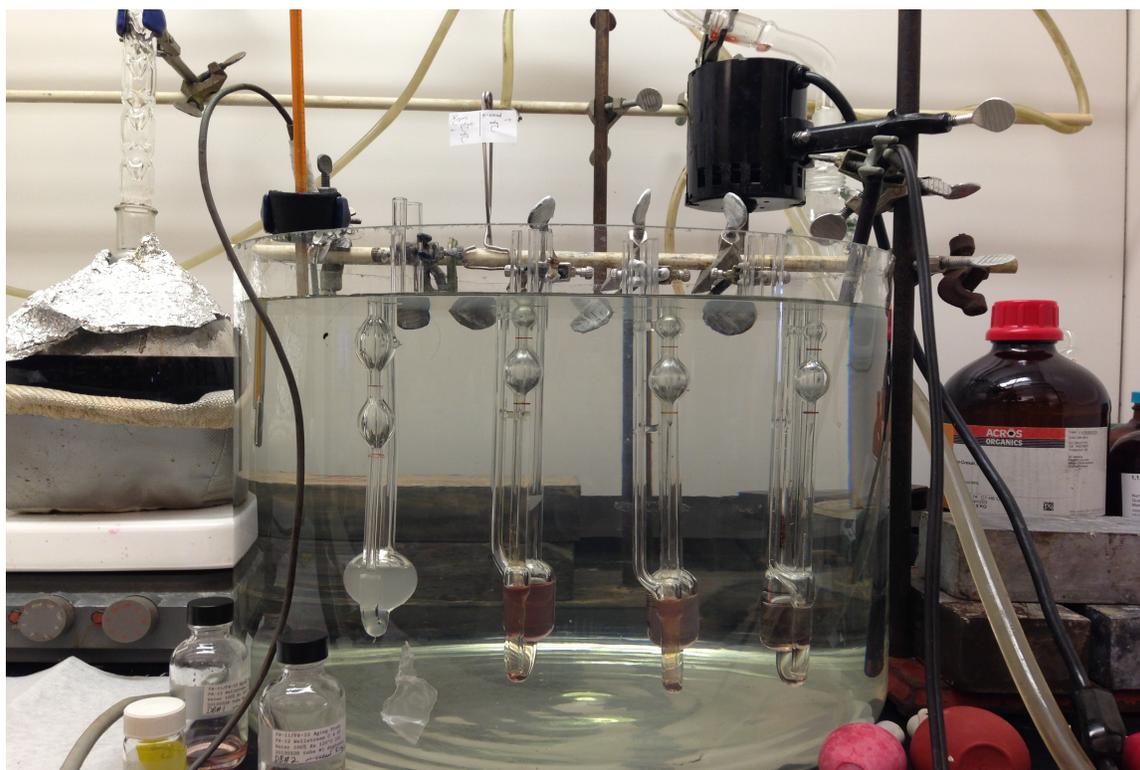

Figure 2.3: Viscosity Bath

2.3 Thermogravimetric Analysis

Thermogravimetric Analysis (TGA) is a technique employed to monitor changes in mass as a function of temperature. The TGA is used to determine the volatile content in polymer samples, a value used to calculate CIV values.

2.3.1 Theory

The TGA instrument is a TA Instruments model G500 TGA. The instrument has a programmable furnace for temperatures up to $1000°C$ with mass measurements to the nearest microgram. The instrument also has gas flow options, which allow for specific control of the environment during heating. In our experiments, we use a constant flow of nitrogen to purge all oxygen in the furnace. At high temperatures, the presence of oxygen would likely result in a combustion reaction as well as significant formation of water and carbon dioxide molecules during heating. The deoxygenated environment prevents these results, which would yield a high percent weight loss, and thus inflate the volatile content determination.

As discussed in the previous section, the volatile content value is necessary to calculate the corrected polymer concentration, and in turn the CIV value. In polymer samples, the volatile content is made up of both water and plasticizer. Plasticizer is an additive frequently used in industry to control and modify mechanical properties and influence viability in specific systems. In the case of poly-amide polymers used in deep water crude pipelines, the plasticizer serves to give the pipeline flexibility. As a polymer ages, the plasticizer content decreases, and the mechanical properties of the polymer are adversely affected. For this reason, plasticizer content can be monitored and quantified as yet another sign of polymer aging.

Different polymer grades have different plasticizer content depending on their intended application; thus, the plasticizer content of polymers is not universal. As the polymer ages, the plasticizer content often decreases and the polymer becomes brittle in a process called "leeching." In our research, we are testing poly-amide 12 polymer grades manufactured by Wellstream and NKT. The two grades are part of a new move to expand PA-12's application in oil pipelines. The TGA procedure we use can be seen in Table 2.1, where the first step prevents the polymer sample from combusting, the second and third steps measure water loss, and the fourth and fifth steps measure plasticizer loss. The percent weight loss at each step can be assumed as the water content and plasticizer content respectively. The sum of these two values is considered the total volatile content of the sample.

Step	Action
1	Select N_2 as the purge gas
2	Ramp 10°C per minute to 105°C
3	Isothermal for 45 minutes
4	Ramp 10°C per minute to 240°C
5	Isothermal for 120 minutes

Table 2.1: TGA method for determining volatile content in PA-11

2.3.2 Sample Preparation

A polymer sample chopped into small pieces of minimal thickness with a razor blade. This creates a large surface area, to ensure that all the volatile content has the opportunity to evaporate. After taring the platinum pan, the sample is loaded and the procedure begins.

The TGA data is collected and analyzed using the TA Universal Analysis Software. The software plots percent weight loss versus time and temperature, as seen in Figure 2.4. The percent weight loss is determined for each isothermal period, the 100°C isotherm for percent water, and the 240°C isotherm for plasticizer.
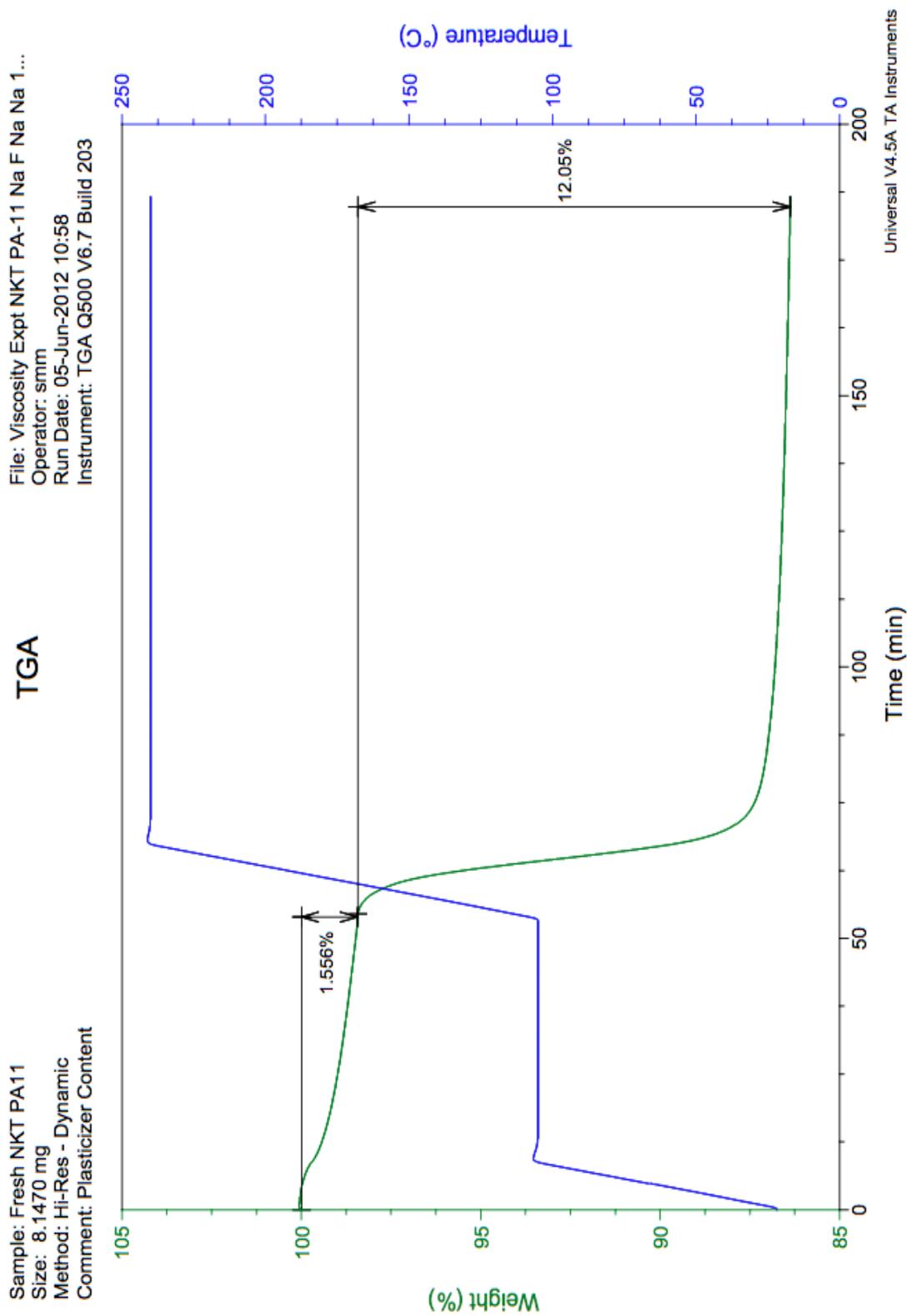
Figure 2.4: TGA Sample Plot

Chapter 3

Methods

3.1 Accelerated Polyamide Aging Hydrolysis

PA-11 and PA-12 display desirable mechanical properties for large diameter crude-oil pipeline applications. PA-11 has been used for many years, and PA-12 has recently been modified for large diameter pipe extrusion. Both PA-11 and PA-12 undergo hydrolysis, seen in Figure 3.1.
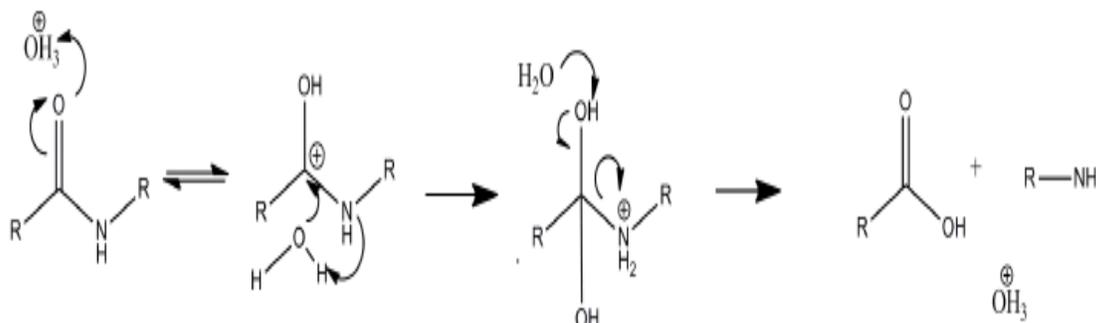

Figure 3.1: Hydrolysis of Poly-Amides

Over the years, the hydrolysis of PA-11 has been well characterized using accelerated poly-amide aging techniques. Due to the recent push to expand polymer resources for crude flexibles, a new grade of PA-12, VESTAMID-L, has been developed and is used by both Wellstream and NKT. It is designed using additives that are not published.

For our PA-11/PA-12 Aging Study Comparison, we are aging PA-11 and PA-12 at three temperatures, 80°C, 100°C, and 120°C, in 100% deionized water (DI Water) of neutral pH, in an

anaerobic environment. These conditions were chosen to best depict the conditions during use of flexible pipe, and to detect any differences in hydrolysis between PA-11 and PA-12. We are considering three samples of polymer in our experiment, PA-11 NKT, PA-12 Wellstream, and PA-12 NKT. These samples were aged in pressure tubes with DI Water, and bubbled with Argon to create the anaerobic environment. This technique has been employed in previous studies to create accelerated poly-amide aging with success. In the field, it might take ten to fifteen years for a polymer to degrade to equilibrium, but in the lab, accelerated aging can be monitored and replicated on the scale of around 300 days. The current theory on molecular weight equilibrium of poly-amides in water of neutral pH was established by Meyer et al. Meyer et al. states that for PA-11 in the 90°C to 135°C range, there is little change in the equilibrium molecular weight regardless of temperature. In addition, Meyer documents that the molecular weight equilibrium is not dependent on the starting molecular weight of the polymer. These findings are important as PA-11 NKT, PA-12 NKT, and PA-12 Wellstream have different starting molecular weights, and will be aged at three temperatures. A single molecular weight equilibrium will be reached for each of the polymer samples, and comparing these equilibria will provide information about the equilibrium reaction kinetics of hydrolysis and recombination. (11)

3.2   Polyamide-11 Hydrolysis Kinetic Fit

The chemical equilibrium equation for poly-amide polymers takes into account the forward hydrolysis reaction, that breaks the amide bond of the poly-amide polymer chain, as well as the reverse recombination reaction, equivalent to the condensation reaction that creates the amide bond between monomer units. This equilibrium is important, as the rate of hydrolysis directly effects the average chain length of a polymer and thus its molecular weight distribution and mechanical properties. The equilibrium equation is seen in Equation 3.1, where R and R' represent alkyl side chains, k_H is the hydrolysis rate constant, k_R is the condensation rate constant (or polymerization rate constant), and where brackets [ ] denote concentration. By using Equation 3.1 the kinetic model needed for determination of k_H and k_R rate constants in solution is shown in Equation 3.2.

From this equation, the assumption that the hydrolysis and condensation rates will eventually reach equilibrium, displayed by Meyer et al., allows us to calculate the k_H and k_R rate constants, seen in Equation 3.3. (11)

$$R'NH_2 + RCO_2H \underset{k_H}{\overset{k_R}{\rightleftharpoons}} R'NCOR + H_2O \tag{3.1}$$
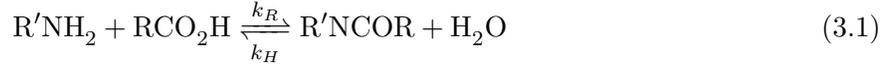
$$\frac{d[R'NH_2]}{dt} = \frac{d[RCO_2H]}{dt} = k_H[R'NCOR][H_2O] - k_R[R'NH_2][RCO_2H] \tag{3.2}$$

$$k_{eq} = \frac{k_R}{k_H} = \frac{[R'NCOR][H_2O]}{[R'NH_2][RCO_2H]} \tag{3.3}$$

The result of applying amide hydrolysis kinetics to polyamide degradation is a logarithmic fit to the average molecular weight degradation with time. $[R'NH_2]$ is the concentration of amine end groups and $[R'CO_2H]$ is the concentration of carboxylic end groups. An increase in the concentration of either end group is indicative of hydrolysis. $[R'NCOR]$ is the concentration of amide bonds and $[H_2O]$ is the concentration of water in the poly-amide matrix.

The concentration of H_2O can be incorporated into the k_H term assuming a large and constant concentration of H_2O. The k_H term is then represented as a pseudo first order rate constant k'_H. Since the hydrolysis of each amide bond yields one carboxyl group, and one amine group, we will assume stoichiometric formation represented in Equation 3.4.

$$\frac{d[R'NH_2]}{dt} = \frac{[RCO_2H]}{dt} = k'_H[R'NCOR] - k_R[RCO_2H]^2 \tag{3.4}$$

Equation 3.4 can be equivalently expressed by Equation 3.5, where x is the amine or acid concentration at time t, and a_o is the initial average number of amide bonds in the polymer sample.

$$\frac{dx}{dt} = k'_H(a_0 - x) - k_R x^2 \tag{3.5}$$

Equation 3.6 is derived from the steady state approximation where x_e represents the equilibrium product concentration. (12)

$$k_R = \frac{k'_H(a_0 - x_e)}{x_e^2} \tag{3.6}$$

Substitution of Equation 3.6 into Equation 3.5 yields Equation 3.7. (12)

$$\frac{dx}{dt} = k'_H(a_0 - x) - \frac{k'_H(a_0 - x_e)}{x_e^2}x^2 \tag{3.7}$$

Separation of variables and integration of Equation 3.7 gives Equation 3.8. (12)

$$\frac{x_e}{(2a_0 - x_e)} \ln\left(\frac{a_0 x_e + x(a_0 - x_e)}{a_0(x_e - x)}\right) = k'_H t \tag{3.8}$$

We are given Equation 3.9, where x is the amine concentration at time t, a_o is the initial number of amide bonds in the starting M_w of the polymer sample, and a is the number of amide bonds at a given M_w under aging conditions. (12)

$$x = a_0 - a \tag{3.9}$$

Similarly, Equation 3.10 represents the same correlation of Equation 3.9 under equilibrium conditions, where x_e is the amine concentration under equilibrium conditions, a_e is the number of amide bonds at equilibrium, and a_o is the initial number of amide bonds in the starting M_w of the polymer sample. (12)

$$x_e = a_0 - a_e \tag{3.10}$$

By substituting Equations 3.9 and 3.10 into Equation 3.8, Equation 3.11 results. (12)

$$\left(\frac{a_0 - a_e}{a_0 + a_e}\right) \ln\left(\frac{a_0^2 - a_e a}{a_0(a - a_e)}\right) = k'_H t \tag{3.11}$$

Rearrangement and substitution of Equation 3.6 yields Equation 3.12.

$$k_R = \frac{k'_H a_e}{(a_0 - a_e)^2} \tag{3.12}$$

Equation 3.13 is used for the final calculations (1; 4), where $M_n = \frac{M_w}{2}$ is assumed for a condensation polymer. This equation allows for the calculation of a, the number of amide bonds in a given molecular weight polymer sample at a time t; a_o is the number of amide bonds in the starting material, a_e is the number of amide bonds in the material once it reaches its aging equilibrium. These terms are a direct function of molecular weight.

$$a = \left(\frac{M_W}{2 \times Monomer\, M_W (g/mol)} \right) - 1 \tag{3.13}$$

Using a least squares fit method and the starting molecular weight of the polymer, the CIV vs. Time data for each sample is fit with a non-linear best fit line. A Matlab program generates a matrix of different k_H and k_R values, and chooses the combination that produces the best fit for the data. This fit is based on equation 3.12, where k_H, k_R, and a_o are used to determine a_e, the concentration of end groups at equilibrium. a_e can then be used to solve for M_{we} using Equation 3.13. The expression for M_{we}, derived from Equation 3.4 at equilibrium, when the concentration of end groups is constant, or d[R'NH_2]/dt=0, is shown in Equation 3.14, in terms of k_H, k_R, $[H_2O]$, and [NH_2], where [NH_2] equals a_e.

$$M_{we} = \frac{k_R [NH_2]^2}{k_H [H_2O]}$$

$$\text{M}_{we} \propto \text{a}_e = [RNCOR]_e$$

$$([RNCOR]_e \text{ from Equation 3.3}) \tag{3.14}$$

Equation 3.15 comes from Equation 3.12, and defines how the k_R/k_H relationship leads to the determination of M_{we}, with quadratic solution shown in Equation 3.16.

$$0 = a_e^2 - (2a_o + k_{eq})a_e - a_o^2 \tag{3.15}$$

$$a_e = \frac{(2a_o + k_{eq}) \pm \sqrt{(-2a_o - 4k_{eq})^2 - 4(a_o)^2}}{2} \tag{3.16}$$

3.2.1   PA-11 vs. PA-12

For PA-12, we cannot at this time determine direct molecular weight via the SEC-MALLS system. In order to apply the general amide hydrolysis kinetic fit model we need molecular weight measurements. Therefore, we will use a secondary method, CIV, to make measurements of the molecular weight. The viscosity measurements are calibrated to molecular weight for PA-11, seen in Figure 3.2, where the molecular weight measurements on the y-axis were measured directly via SEC-MALLS, and the CIV values on the x-axis. The exponential curve best fit is represented by Equation 3.17. Plotting the natural log of this data yields a linear best fit line depicted in Equation 3.18 in the form of y=ax+b, where y is $ln(M_w)$ at a given CIV. The fitting parameter constants a and b are representative of PA-11. We will assume that PA-12 has the same fitting parameters as PA-11, such that we can estimate the average M_w of a PA-11 and PA-12 sample using its measured CIV. Using the estimated M_w measurements for PA-11 and PA-12 from CIV determination, we can apply the general amide hydrolysis kinetic fit model discussed in Section 3.1.

$$M_w = e^{1.9ln(CIV)+10.2} \tag{3.17}$$

$$ln(M_w) = 1.9ln(CIV) + 10.2 \tag{3.18}$$

Thus, for PA-12, a relative viscosity measurement is taken for a given polymer sample, see Equation 2.1. That relative viscosity is used to determine the corrected intrinsic viscosity value (CIV) of that sample, see Equation 2.5. For PA-12 we assume that the added elastomer has no affect on solution viscosity. Once the CIV is determined for PA-12, the molecular weight of the sample is estimated using the M_w vs. CIV fit for PA-11. These estimated M_w values are then used to create the general amide hydrolysis kinetic fit model, which generates k_h, k_R, and $M_{w equilibrium}$ values. From these values, Arrhenius plots are used to determine activation energies for hydrolysis and recombination.

For PA-11, the process is the same. However, the SEC-MALLS measures the molecular weight

of PA-11 NKT samples directly. The SEC-MALLS calibrates the M_w vs. CIV fit, that can then be applied to the secondary method CIV measurements of PA-11 and PA-12.
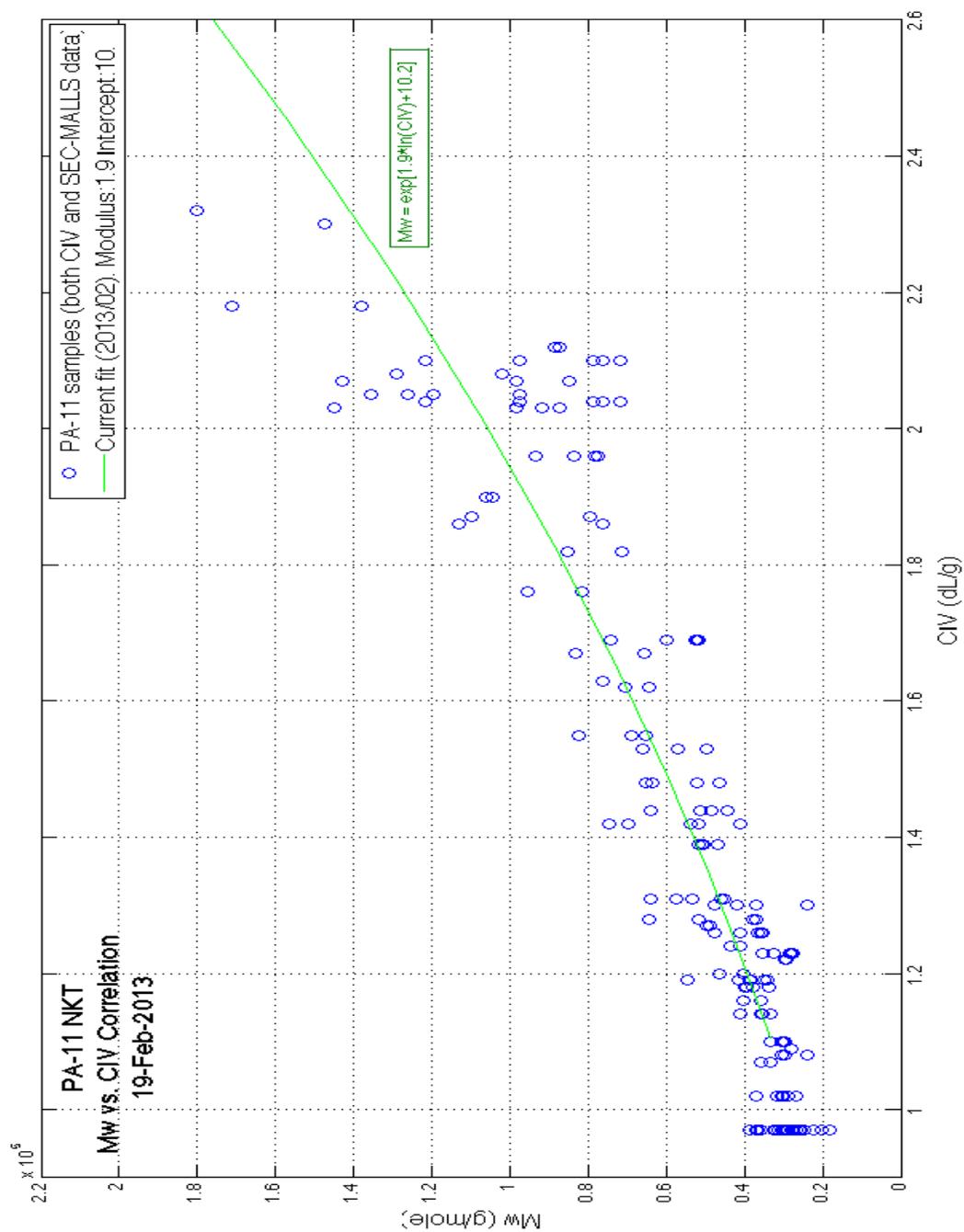
Figure 3.2: M_w vs. CIV Correlation for PA-11 using both SEC-MALLS data and CIV data. Plotting the natural log of this data yield a linear best fit line displayed in Equation 5.1.

Chapter 4

Results

The CIV data taken for the three polymer samples at each temperature are plotted as a function of time in Figures 4.1 - 4.3. Each figure represents a different polymer sample at all three temperatures, PA-11 NKT is depicted in Figure 4.1, PA-12 Wellstream in Figure 4.2, and PA-12 NKT in Figure 4.3. The kinetic best fit lines are displayed for each temperature, with the exception of the 80°C data for PA-12 Wellstream and PA-12 NKT. These 80°C fit lines are omitted because the samples have not yet reached equilibrium. The best fit line for PA-12 NKT is an extrapolation based on the assumption that PA-12 NKT and PA-12 Wellstream will reach the same M_{we} for each temperature irrespective of starting molecular weight; this assumption is verified by a comparison of the 120°C data for PA-12 NKT and PA-12 Wellstream data in Figure 4.5.

Figures 4.4 and 4.5 represent the same CIV vs. Time relationships from the previous figures, but these figures are grouped by temperature instead of by polymer sample, Figure 4.4 depicts the 100°C data, and Figure 4.5 the 120°C.

In agreement with Meyer et al., our CIV vs. Time plots, Figures 4.1-4.5, show each polymer sample approaching an equilibrium molecular weight. (11) In contrast to Meyer, our study shows that the equilibrium molecular weight reached for each sample is dependent on temperature; with the higher temperature resulting in a lower equilibrium molecular weight, Figures 4.1 - 4.3.
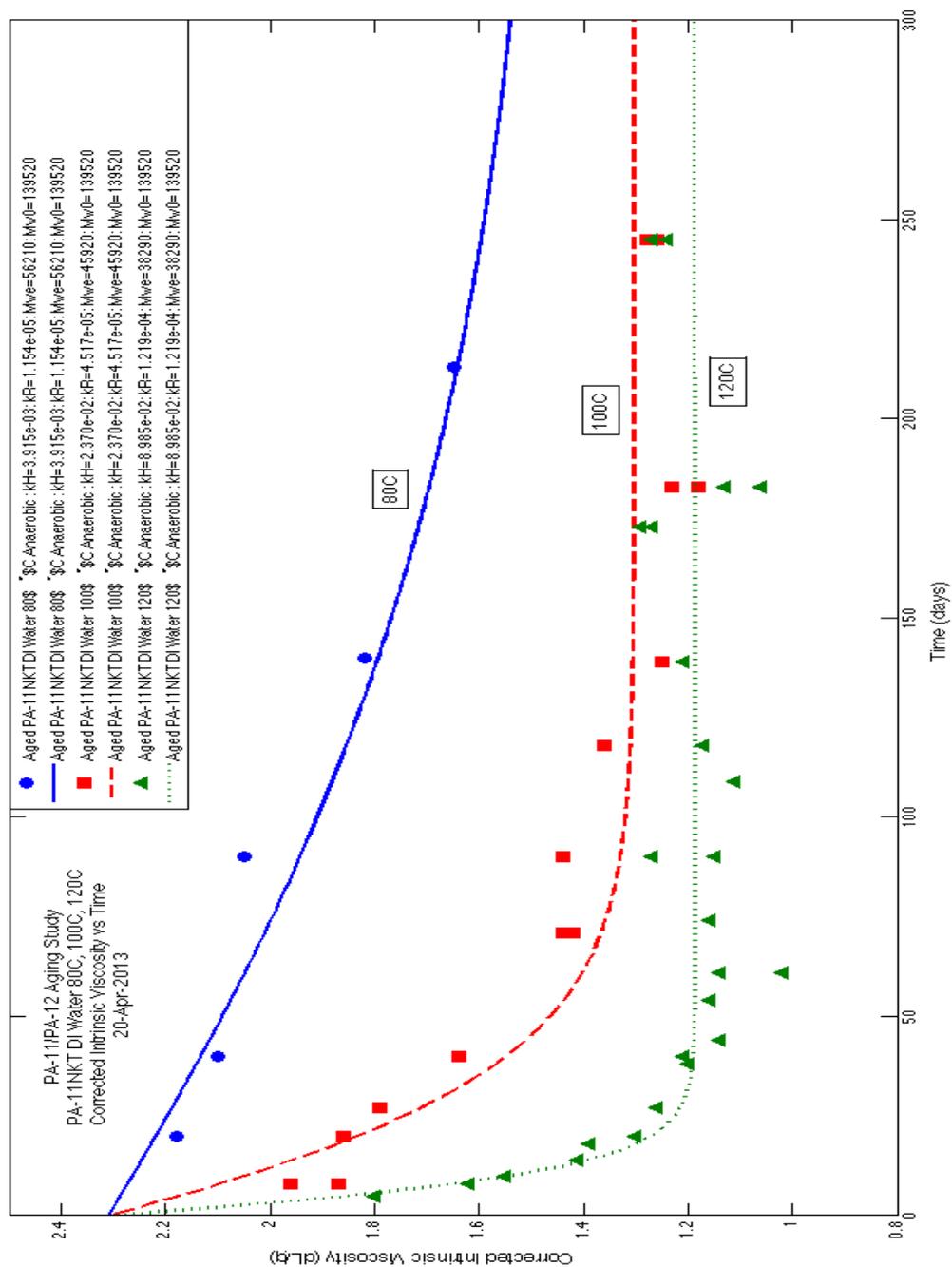
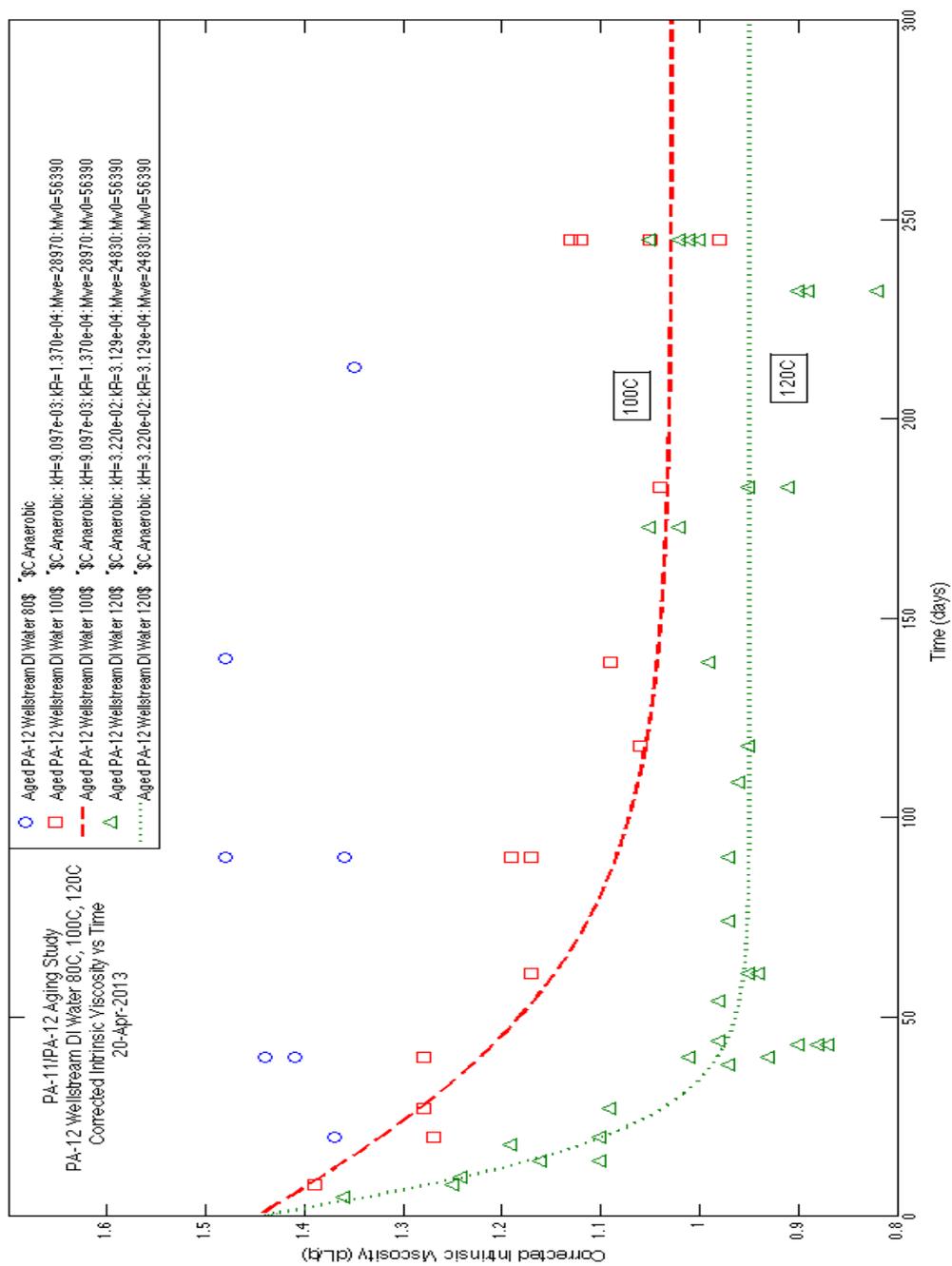Figure 4.1: PA-11 NKT 80C, 100C, 120C; CIV vs. Time

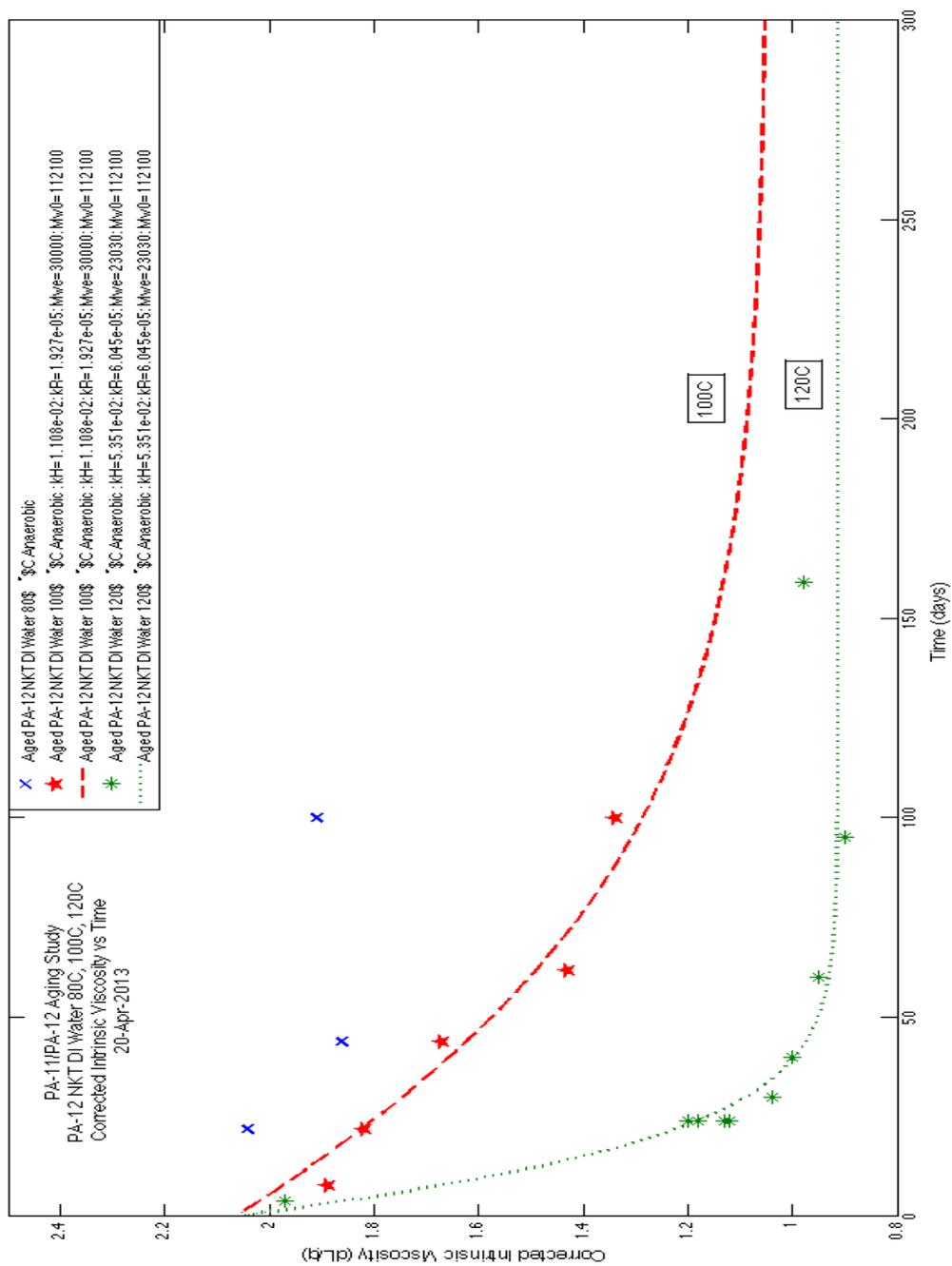Figure 4.2: PA-12 Wellstream 80C, 100C, 120C; CIV vs. Time

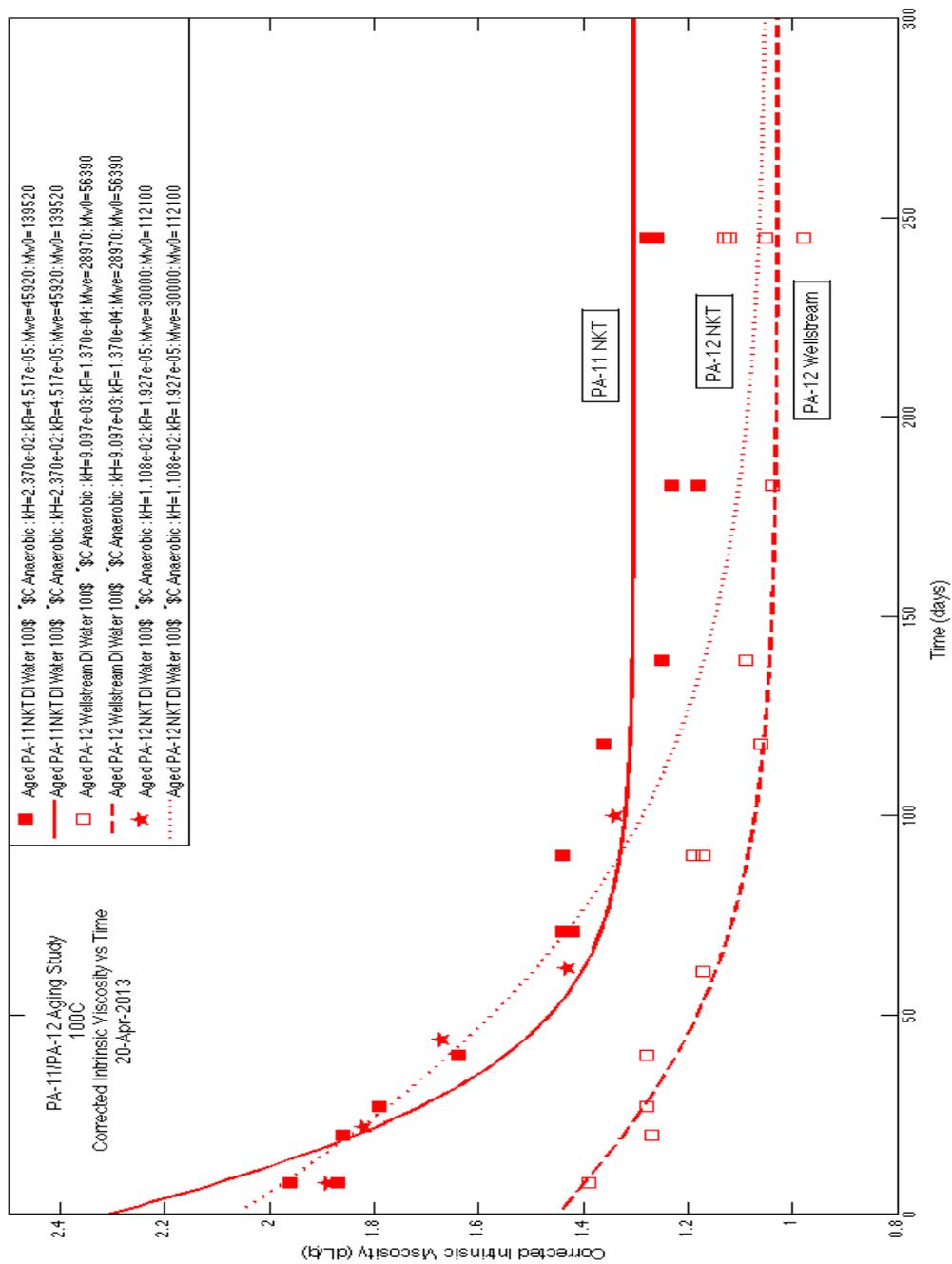Figure 4.3: PA-12 NKT 80C, 100C, 120C; CIV vs. Time

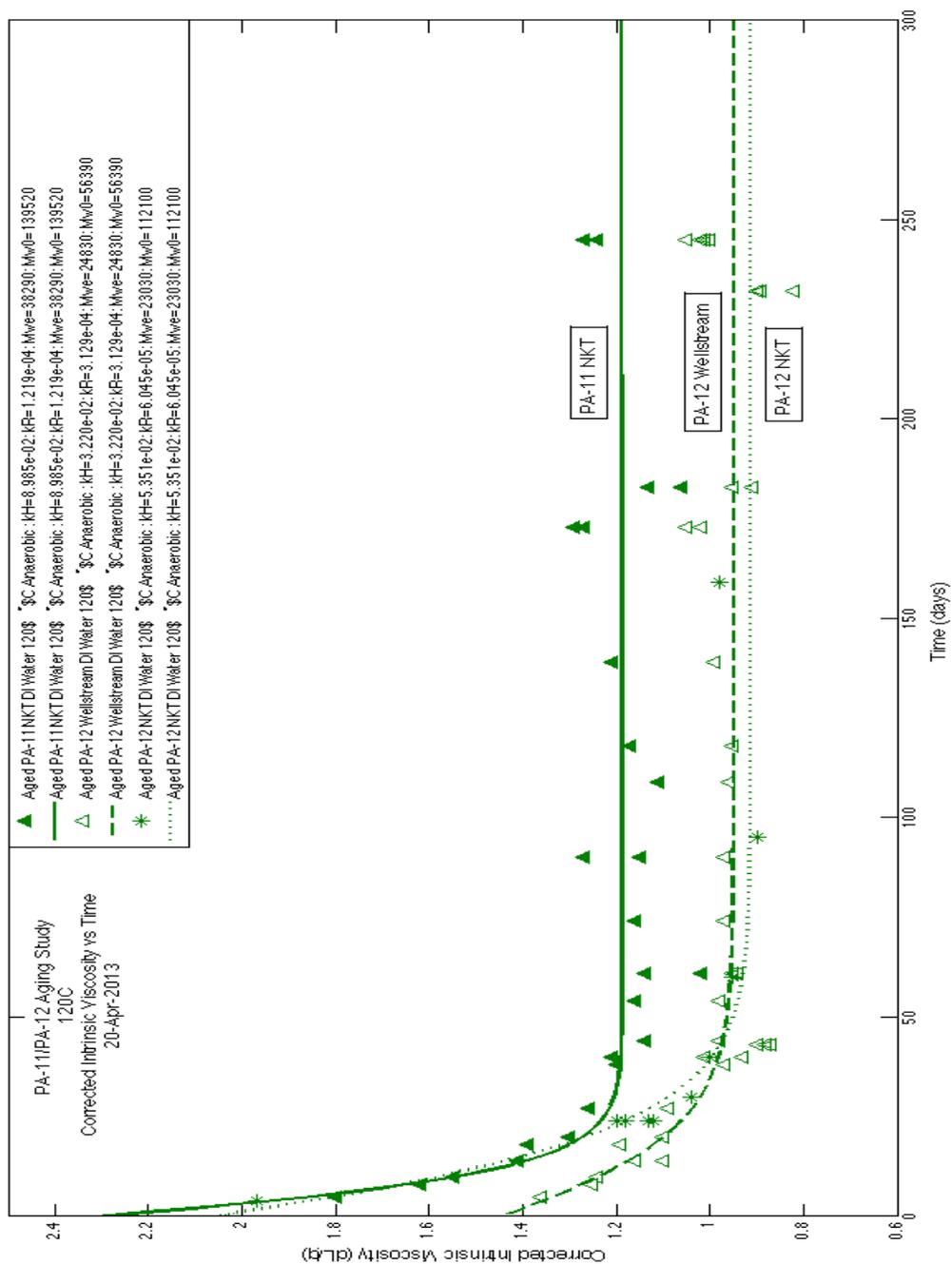Figure 4.4: 100C PA-11/PA-12 Aging Study; CIV vs. Time

Figure 4.5: 120C PA-11/PA-12 Aging Study; CIV vs. Time

Chapter 5

Discussion

As shown in Equation 3.12, a_e, the number of amide bonds at equilibrium, is dependent on two parameters, k_H and k_R. This dependence is based on the assumption that water is in excess in the equilibrium system, Equation 3.4. From this assumption, we can calculate a_e, and convert to M_{we}, again using Equation 3.13. M_{we} allows for determination of the relationship between $[NH_2]$ and $[H_2O]$ at equilibrium, Equation 3.14. Table 5.1 presents the k_H, k_R, k_{eq}, M_{we}, and M_{wo} for all three polymer samples at 80°C, 100°C, and 120°C.

An Arrhenius plot, $\ln[k_H]$ vs. $1/T$, where T is the temperature in Kelvin, and k is the reaction rate constant, is represented by Equation 5.1. Using k_H, hydrolysis rate constant, and T, temperature, we can determine the energy of activation for the hydrolysis reaction using the slope of an Arrhenius Plot, $\ln(k_H)$ vs. $\frac{1}{T}$. The same procedure is also applied to k_R and M_{we}.

$$ln(k) = [(\frac{-E_a}{R})(\frac{1}{T}) + ln(A)]$$

k = rate constant, R = gas constant (J/molK), T = temperature (K), A = Arrhenius constant, E_a = activation energy (J/mol) (5.1)

Sample	Temp.	k_H	k_R	$k_{eq} = \frac{k_R}{k_H}$	$M_{wInitial}$	$M_{wEquil.}$
PA-11 NKT	80C	3.915e-3	1.154e-5	2.9e-3	139,520	56210
	100C	2.370e-2	4.517e-5	1.9e-3	139,520	45,920
	120C	8.985e-2	1.219e-4	1.4e-3	139,520	38,290
PA-12 Wellstream	80C	-	-	-	56,390	-
	100C	9.097e-3	1.370e-4	1.5e-2	56,390	28,970
	120C	3.220e-2	3.129e-4	9.7e-3	56,390	24,830
PA-12 NKT	80C	-	-	-	112,100	-
	100C	1.108e-2	1.927e-5	1.7e-3	112,100	30,000
	120C	5.351e-2	6.045e-5	1.1e-3	112,100	23,030

Table 5.1: k_H, k_R, k_{eq}, M_{wo} and M_{we} for PA-11 NKT, PA-12 Wellstream, and PA-12 NKT. As discussed in Chapter 4, the 80°C kinetic fit lines were omitted.

The Arrhenius Plots for k_H and k_R can be seen below in Figures 5.2 and 5.3 respectively. The slope of the linear fit of this data is set equal to $-E_a/R$, and the activation energy of hydrolysis and recombination was determined for PA-11 NKT, PA-12 Wellstream, and PA-12 NKT, Table 5.2. The activation energies determined for PA-11 NKT in 100% DI Water in this study are in agreement with the values determined by Meyer et al. and Dr. Jaeton Glover. (11; 1)

	E_a(kJ/mole)		
Sample	k'H	k'R	E_a(k$_H$)-E_a(k$_R$)
PA-11 NKT (CIV)	91 ± 9	68 ± 25	23
PA-12 Wellstream (CIV)	77 ± 9	50 ± 25	27
PA-12 NKT (CIV)	96 ± 9	70 ± 25	26

Table 5.2: Activation Energies calculated using the slope of ln(k) vs.1/T Arrhenius Plot.
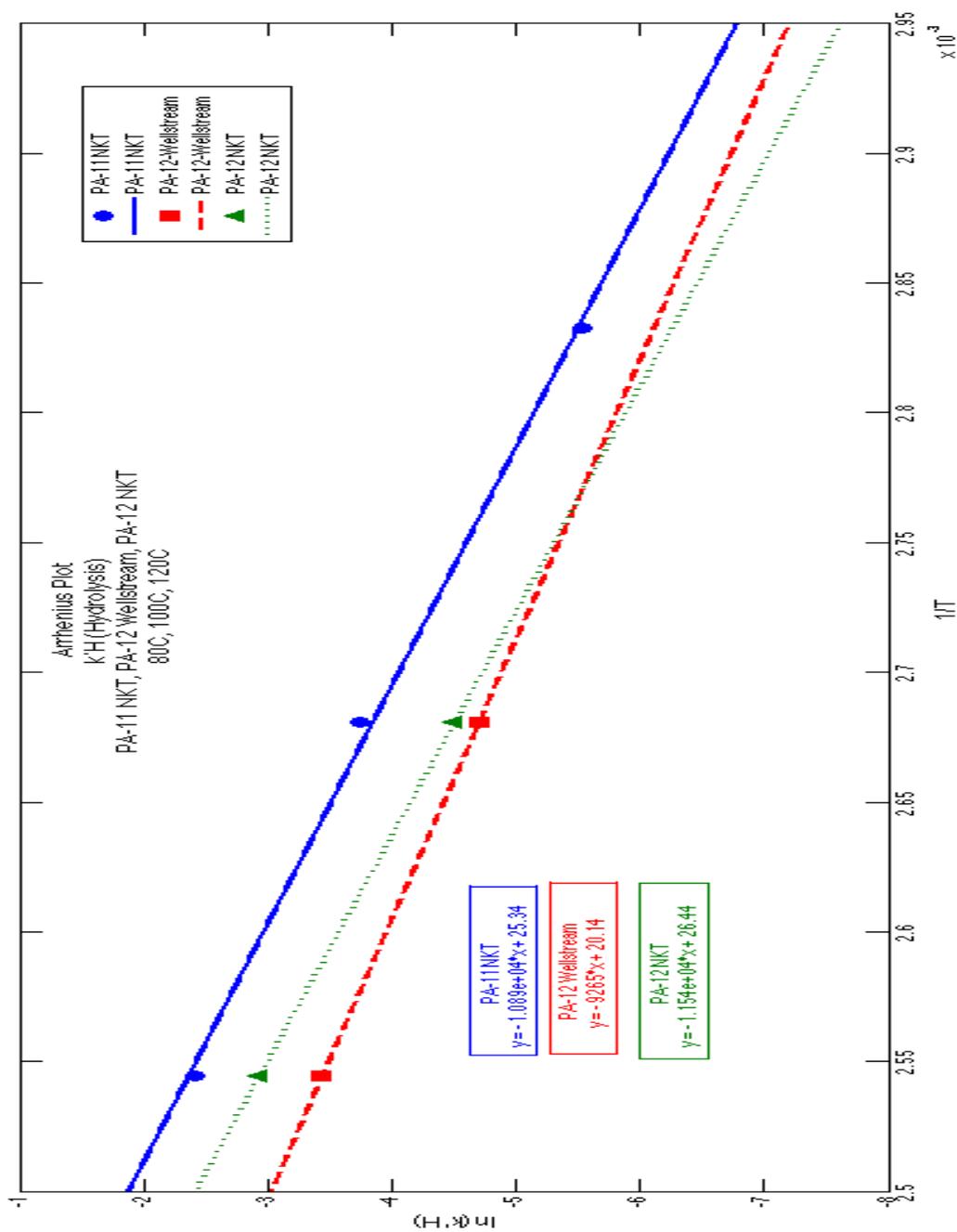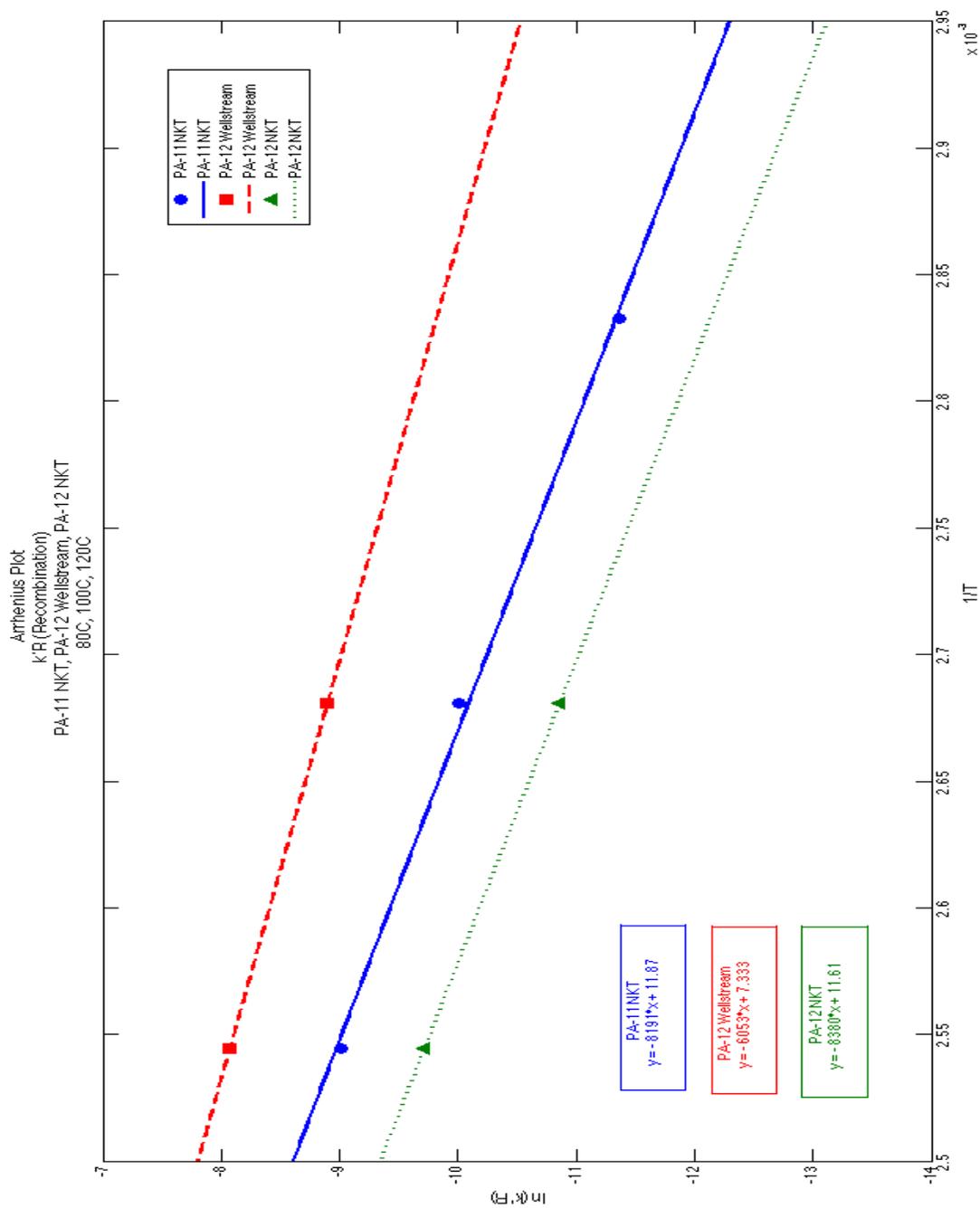
Figure 5.1: k'H Arrhenius Plot PA-11 and PA-12

Figure 5.2: k'R Arrhenius Plot PA-11and PA-12

The most important relationship in our analysis is the relationship of M_{we} to k_H and k_R. As seen in Table 5.1, the initial molecular weight of the polymer has a large impact on how long it takes the polymer to reach its equilibrium molecular weight, but not the final value of the equilibrium molecular weight. PA-12 NKT for example has an M_{wo} that is 56,000 g/mol higher than PA-12 Wellstream, yet they both reach approximately the same equilibrium molecular weights for the 120°C samples. Our data shows that M_{we} is temperature dependent, in contrast to Meyer et al. (11), but not dependent on M_{wo}.

Both k_H and k_R showed temperature dependence in all three polymer samples. As temperature increased, the k_H and k_R values also increased. For PA-12 Wellstream, the k_H and k_R values are smaller in comparison to PA-11 NKT and PA-12 NKT, but this is attributed to the higher starting molecular weight of the NKT samples. The starting molecular weight of PA-12 Wellstream is in the curved region of the aging trend, and does not experience the same linear k_H dominance early in aging as seen with higher M_{wo} samples. For this reason, it is harder to separate out the k_H and k_R values using our fit model for PA-12 Wellstream, as no process, hydrolysis or recombination, is overly dominant at its starting molecular weight.

A better comparison is achieved using the PA-11 NKT and PA-12 NKT samples, as their starting molecular weights are more similar. The rates of hydrolysis and recombination are definitely slower for PA-12 in these samples. In addition, PA-12 exhibits a lower molecular weight equilibrium relative to PA-11 at all temperatures, Figures 4.4 and 4.5. To explain this fact, we examined the k_{eq} value, defined in Equation 3.14, where M_{we} is proportional to the ratio of k_R over k_H. The k_{eq} values showed a correlation to M_{we} such that M_{we} decreased as the k_{eq} value decreased, Table 5.1. This can be explained by the decrease in relative rate of recombination, or increase in relative rate of hydrolysis, with a decrease in k_{eq}. The k_{eq} values for PA-12 NKT were lower at all temperatures in comparison to PA-11 NKT.

The activation energy analysis, Table 5.2, depicts relatively similar energies of activation for PA-11 and PA-12. The outlier in this analysis is the PA-12 Wellstream data, but as discussed before, the k_H and k_R values for PA-12 Wellstream are not as reliable, as the fit model breaks down at

lower starting molecular weights. The difference between the activation energies of hydrolysis and recombination, seen in the third column of Table 5.2 shows a slightly greater difference for PA-12 in comparison to PA-11, but this is within the experimental error. The similarity in the PA-12 NKT difference, 27 kJ/mole, and the PA-12 Wellstream difference, 26 kJ/mole is fortuitous. The similarity in activation energies for PA-11 and PA-12 show similar temperature dependence for PA-12 relative to PA-11, although the non-logarithmic factor is different for the two polymers.

It was our hypothesis, that because PA-12 has less uptake of water than PA-11 (7; 8), PA-12 will undergo a slower rate of hydrolysis in comparison to PA-11 in the same conditions. Our data shows that PA-12 NKT does in fact have a slower rate of hydrolysis, k_H, relative to PA-11 NKT at all temperatures. PA-12 also has a slower rate of recombination at all temperatures. The differences in the k_H and k_R values for PA-11 and PA-12 are probably influenced by the relative size of molecules in PA-11 vs. PA-12. However, the differences in k_H and k_R for PA-11 and PA-12 do not directly explain differences in the values of M_{we}. M_{we} is dependent on the ratio of k_R to k_H, as well as the ratio of [NH_2] to [H_2O]. PA-12 NKT does reach a lower M_{we} at all temperatures in part due to a lower k_{eq} value. However, as we also saw, with the Arrhenius workup, PA-12 and PA-11 have very similar activation energies for hydrolysis and recombination and temperature dependence.

Chapter 6

Conclusion

Our initial hypothesis suggested that we would see a difference in hydrolysis rates between PA-11 and PA-12 because PA-12 absorbs less water. (7; 8) We saw slower rates of hydrolysis and recombination for PA-12 relative to PA-11 for all temperatures. The equilibrium molecular weight was also lower for PA-12 at all temperatures, a function of the k_{eq} value. We showed definite M_{we} dependence on temperature in contrast to Meyer et al, as well as equilibrium independence of starting molecular weight

Our original hypothesis has been modified, as the difference in rate of hydrolysis for PA-12 does not explain its lower equilibrium molecular weight. A combination of complex factors, k_H, k_R, [NH_2], and [H_2O], determine equilibrium molecular weight as seen in Equation 3.14. Our current work characterizes the influence of k_H and k_R values.

Our findings are important to our current understanding of PA-11 and PA-12, as well as to future work and environmental and mechanical evaluation. An understanding of hydrolysis kinetics, and the differences between PA-11 and PA-12 will provide insight into the mechanical properties of both polymers in aging environments. Meyer et al. proved that molecular weight is the best way to monitor mechanical viability of aged polyamide polymers, and thus our understanding of M_{we} in accelerated aging conditions can be combined with the mechanical data to develop design factors for PA-12 in large diameter crude riser applications. It is well within reason to assume that the industrial design factor for PA-11 and PA-12 will not be the same with respect to CIV, but that data remains incomplete. It is clear that an understanding of hydrolysis kinetics will lay

the foundation for a determination of PA-12 industrial design factors. PA-11, due to its wide use and characterization can serve as a model for experimentation and reference as polymer chemists continue to work characterizing PA-12 for use in crude-oil deep water risers.

Bibliography

[1] A. J. M. Glover, Characterization of pa-11 flexible pipe liner aging in the laboratory and in field environments throughout the world, Doctor of philosophy, The College of William and Mary, Williamsburg, VA USA (2011).

[2] S. Buchner, *et al.*, *26th International Conference of Offshore Mechanics and Arctic Engineering* **1**, 711 (2007).

[3] G. Hochstetter, P. Dang, *Proceedings of the ASME 2009 28th International Conference on Ocean, Offshore and Arctic Engineering*, ASME, ed. (ASME, 2009), pp. 797–803.

[4] J.-A. S. Hocker, The role of small carboxylic acids during poly(amide) 11 hydrolysis, Master of science, The College of William and Mary, Williamsburg, VA USA (2012).

[5] E. Rosenthal, U.s. to be worlds top oil producer in 5 years, report says, New York Times (2012). Http://www.nytimes.com/2012/11/13/business/energy-environment/report-sees-us-as-top-oil-producer-in-5-years.html.

[6] K. Galbraith, Deep-sea drilling muddies political waters, New York Times (2013). Http://www.nytimes.com/2013/02/07/business/energy-environment/07iht-green07.html.

[7] A. P. Institute, Api technical bulletin tr17rug, 1st edition, *Bulletin TR17RUG*, API (2002).

[8] A. Incorporated, *Rilsan PA-11: Created from a Renewable Source*, Arkema Incorporated, 4/8, cours Michelet - 92800 Puteaux (France).

[9] S. D. K. K., *Operation Manual for Shodex PAK GPC HFIP-800 Series.*, Shodex, Tokyo, Japan, manual no. 840 edn. (2010).

[10] H. R. Allcock, F. W. Lampe, J. E. Mark, *Contemporary Polymer Chemistry* (Pearson Education (Prentice-Hall) Inc, Upper Saddle River, NJ, 2003), third edn.

[11] A. Meyer, N. Jones, Y. Lin, D. Kranbuehl, *Macromolecules* **35**, 2784 (2002).

[12] K. J. Laidler, *Chemical Kinetics* (Harper & Row, New York, NY, 1987), third edn.